

Chapter 1: Introduction*

1.1 Overview: Inorganic Complexes as Chemotherapeutic Agents

The serendipitous discovery of the anticancer properties of *cis*-dichlorodiammineplatinum (II) (cisplatin) in 1965 played an integral role in the birth of medicinal inorganic chemistry as a field.¹⁻⁵ Metal complexes, previously considered to be simply toxic, could now be applied strategically to inhibit the rapid cell division of malignant cancers. For many years, the field focused on the development of more potent analogues, mainly in the form of second and third generation derivatives of cisplatin, leading to the FDA approval of two additional *cis*-platinum(II) complexes, carboplatin and oxaliplatin (**Figure 1.1**).^{2,3} Cisplatin and carboplatin, in particular, have been highly successful in the treatment of a variety of cancers, including testicular, ovarian, cervical, and non-small cell lung cancers.⁴ However, these treatments are often associated with severe side effects and a build-up of resistance. These issues have led researchers to focus more recently on the development of novel non-platinum chemotherapeutics.

The rich photophysical and photochemical properties of metal complexes, in addition to their basic coordination chemistry, make them ideal scaffolds for a wide variety of biological applications. Though the pharmaceutical industry in general has shied away from “heavy metal” therapeutics, with the exception of cisplatin and its derivatives, there are in fact real opportunities in the development of transition metal pharmaceuticals, given their high modularity, ease of synthesis in preparing molecules of complex shapes and

*Adapted from Weidmann, A. G.; Komor, A. C.; Barton, J. K. Targeted Chemotherapy with Metal Complexes. *Comments in Inorg. Chem.* **2014**, *34*, 114-123. DOI: 10.1080/02603594.2014.890099.

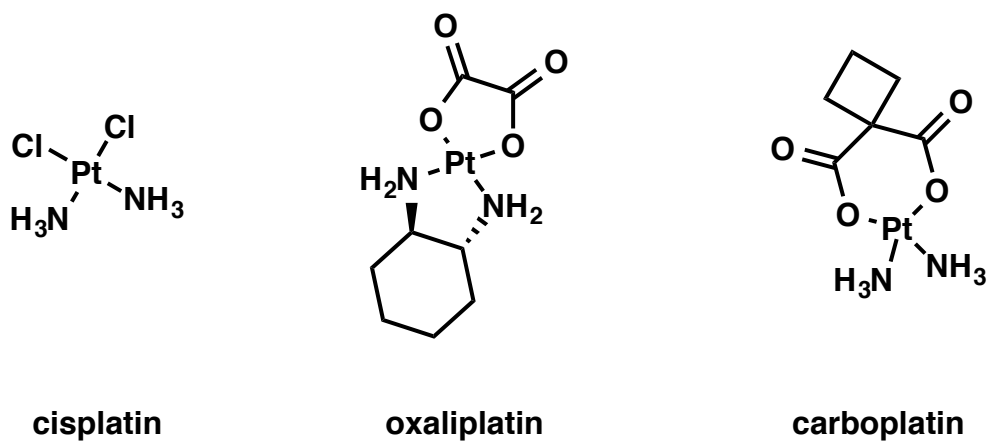


Figure 1.1 Chemical structures of classical, FDA-approved platinum-based chemotherapeutics.

symmetries, and the ability to monitor their fate within the cell using a variety of spectroscopies.

The traditional focus of many laboratories has been in the development of more potent metal complexes that function like cisplatin in coordinating to DNA but are more effective, either because of more optimum uptake characteristics, or the inability of lesions formed to be easily detected and repaired. Much time and attention have been spent in this arena. However, the goal has moved also to the design of complexes with a new strategy based upon selectivity, with the preparation of transition metal complexes that are more selective than cisplatin owing to a design strategy where the complex interacts with a specific biological target found prominently in cancer cells.

1.2 Platinum-Based Chemotherapeutics

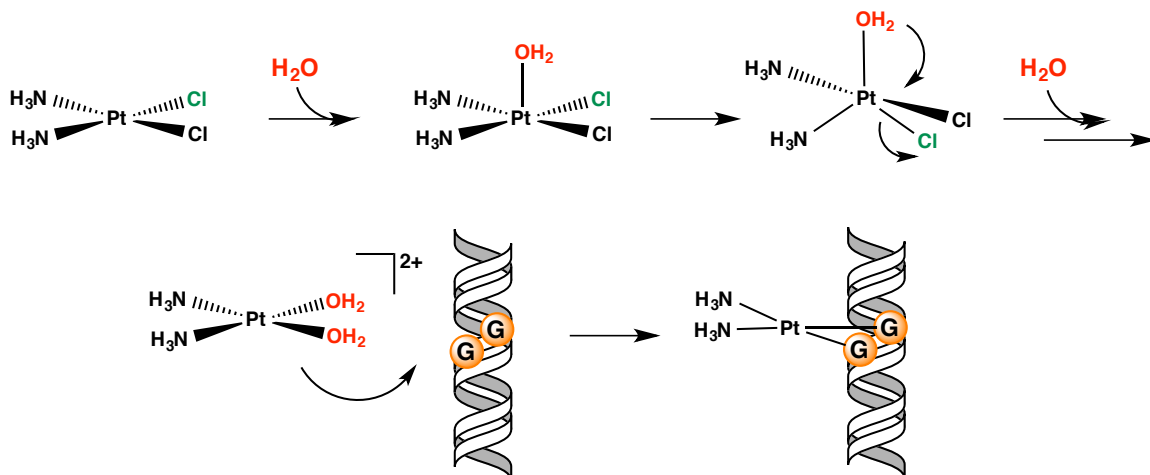
1.2.1 Mechanism of *Cis*-platinum (II) Activity

The anticancer properties of cisplatin and its analogues arise primarily from their ability to covalently bind DNA. In the case of cisplatin, the *cis*-chloride ligands remain largely inert in an extracellular environment, where the salt concentration is high ($[Cl^-] = 100 \text{ mM}$). Once inside the cell, the chloride concentration decreases approximately 25 fold.^{5,6} Cisplatin then becomes aquated via a reversible associative ligand substitution mechanism, driven forward by the reduced intracellular chloride concentration.⁵ The subtle hydrolysis kinetics of cisplatin are critical to its efficacy and distinguish it from its clinically ineffective stereoisomer, transplatin. The *trans* effect labilizes the chloride ligands of transplatin, deactivating the complex before it can achieve potency.⁷ In contrast, the resulting *cis*- $[Pt(NH_3)_2(OH_2)_2]^{2+}$ is a potent electrophile that readily reacts with various biological ligands, but its primary therapeutic target is DNA. In particular, cisplatin

forms crosslinks at the *N7* position of guanine residues, which is the most nucleophilic site on DNA (**Scheme 1.1**). Due to the presence of two *cis*-labile ligands, *cis*-platinum complexes generally form 1,2- and 1,3-intrastrand crosslinks – known as “bifunctional” adducts – with guanine residues in the major groove, which account for more than 90% of *cis*-platinum-DNA adducts in the cell.⁴

Platinum adducts severely distort DNA through helical unwinding and bending; in the case of cisplatin, 1,2-intrastrand crosslinks bend the duplex up to 60° toward the major groove, exposing a wide and shallow minor groove. Several classes of proteins, including those involved in DNA repair, recognize this lesion, triggering a variety of biological responses.⁵ For example, proteins involved in the correction of DNA base pair mismatches, known as the mismatch repair (MMR) pathway, bind cisplatin-DNA adducts and attempt, unsuccessfully, to initiate repair. The inability of repair enzymes to fix the damaged DNA leads to inhibition of transcription and DNA synthesis, as platinated residues cannot be properly replicated.^{4,5} This in turn causes cell-cycle arrest and, ultimately, cell death by apoptosis.⁸ As a result, *cis*-platinum (II) activity is most potent in rapidly dividing cells, such as those involved in carcinogenesis.

In some cases, platinum adducts are recognized by proteins that are able to excise the lesion and thus repair the DNA. For instance, nucleotide excision repair (NER) proteins, which recognize and repair DNA damage that distorts the helix, are able to successfully restore crosslinked DNA to its original state, leading to cisplatin resistance.⁹⁻¹¹ In cisplatin-sensitive cells, platinum adducts are often recognized first by alternative proteins, such as high mobility group (HMG)-domain proteins, which shield the lesions from binding and repair by the NER pathway.^{12,13}



Scheme 1.1 Thermal activation of cisplatin via associative substitution of the labile chloride ligands with water molecules. The resulting cisplatin di-aqua complex is a potent electrophile that reacts readily with DNA, preferentially forming 1,2-intrastrand cross-links with nucleophilic guanine residues (represented by “G” in the orange circles) at the *N7* position.

Cisplatin resistance can arise through recognition and repair of Pt-DNA lesions, as is the case with NER, or through the absence of proteins that process these adducts and induce cell death. Cancers that are deficient in the MMR pathway are generally resistant to cisplatin;^{14,15} the futile cycle of recognition and attempted repair of platinum adducts by MMR proteins is postulated to trigger a signaling cascade that initiates apoptosis.⁴ In cancers that are MMR-deficient, these signaling events do not occur or do so improperly, and thus cells evade cisplatin-induced apoptosis and continue to proliferate. Indeed, loss of MMR proficiency increases the rate of development of resistance to cisplatin 1.8 fold, and MMR-deficiencies are found in 80% of hereditary nonpolyposis colorectal carcinomas and 16% of all solid tumors.^{14,16} Treatment of MMR-deficient cancers with cisplatin can be potentially devastating, in fact, as the preferential targeting of healthy MMR-proficient cells selects for and enables the continued proliferation of the malignant phenotype.

1.2.2 Cisplatin Derivatives and Analogues

In addition to the previous examples, there are many classes of proteins that bind and process cisplatin adducts in DNA and, as a result, many sources of inherent and acquired resistance. Cisplatin resistance can also arise from cellular efflux or deactivation of the drug through off-target binding.¹⁷ Furthermore, cisplatin causes notoriously severe side effects, including kidney failure (nephrotoxicity), nervous system damage (neurotoxicity), hearing loss (ototoxicity), and bone marrow suppression (myelotoxicity).¹⁸ Much effort has been focused on the development of derivatives to overcome the clinical limitations of cisplatin.

To date, thousands of platinum-based anticancer complexes have been synthesized and studied; however, only two have passed clinical trials and been approved for use by the FDA: carboplatin and oxaliplatin (**Figure 1.1**).¹⁸ Despite the limited success of platinum derivatives, a strict structure activity relationship (SAR) had evolved, claiming that *cis*-coordination of two monodentate or one bidentate labile ligand(s) to a platinum (II) center in a square planar geometry was essential for anticancer activity.¹⁹

The FDA-approved therapeutics carboplatin and oxaliplatin follow this classical SAR pattern. Carboplatin contains a bidentate cyclobutanedicarboxylato leaving group ligand and two *cis*-ammine non-leaving group ligands. The dicarboxylate ligand alters the activation kinetics of aquation, reducing side effects and off-target toxicity. The active form of carboplatin, *cis*-[Pt(NH₃)₂(OH)₂]²⁺, is identical to that of cisplatin, however, and forms the same DNA adducts. As a result, carboplatin mitigates the side effects of cisplatin but does not offset resistance.^{19,20}

Oxaliplatin also contains a bidentate oxalate leaving group ligand, but has a bidentate *trans*-(R,R)-1,2-diaminocyclohexane non-leaving group ligand in lieu of free amines.² The covalent adducts formed by oxaliplatin are chemically distinct from that of cisplatin and carboplatin, although it still preferentially binds at d(GpG) sites to form 1,2-intrastrand crosslinks. The distortions to the DNA duplex as a result of oxaliplatin binding are less severe than those of cisplatin, and the hydrogen bonding contacts between the inert amine ligand and the DNA backbone are altered.²¹ As a result, the oxaliplatin-DNA adduct is not recognized by the same proteins that process cisplatin-DNA, including those involved in MMR, and is instead processed by orthogonal biological

pathways.²² Consequently, oxaliplatin displays little cross-resistance with cisplatin and is typically a first-line therapy for MMR-deficient cancers.²³

Over the years, syntheses of platinum complexes have strayed from the restrictive SAR rules to afford octahedral Pt(IV) centers,²⁴ monofunctional Pt(II) complexes containing *N*-heterocyclic ligands,²⁵ *trans*-platinum (II) complexes,²⁶ and many others. Variations in the leaving and non-leaving ligand sets, geometries, and oxidation states have allowed for tunable platinum therapeutics that are highly potent and often exhibit little cross-resistance with cisplatin in many cancerous cell lines. However, the primary mechanism by which these complexes function remains fundamentally the same – that is, they form covalent crosslinks with genomic DNA to interfere with replication, transcription, and mitotic processes to trigger cell death by apoptosis. In this way, cisplatin and its analogues are known as “classical” chemotherapeutics: they achieve potency by damaging cancer cells *more* than healthy cells, yet possess no real mechanism for avoiding healthy cells entirely. For these reasons, research efforts in recent years have shifted towards the development of targeted chemotherapy.

1.3 Targeted Chemotherapy with Metal Complexes

In “targeted” therapy, a drug is developed to target a specific cellular signaling pathway on which cancer cells depend for growth, metastasis, or angiogenesis.²⁷ These types of compounds aim to damage cancer cells *instead* of healthy cells. Targeted therapy focuses on the development of selective therapeutics, whereas classical therapy has focused on the development of increasingly cytotoxic compounds. The next generation of chemotherapeutics has focused on targeting biomolecules, including proteins, organelles, and specific DNA lesions (**Figure 1.2**).

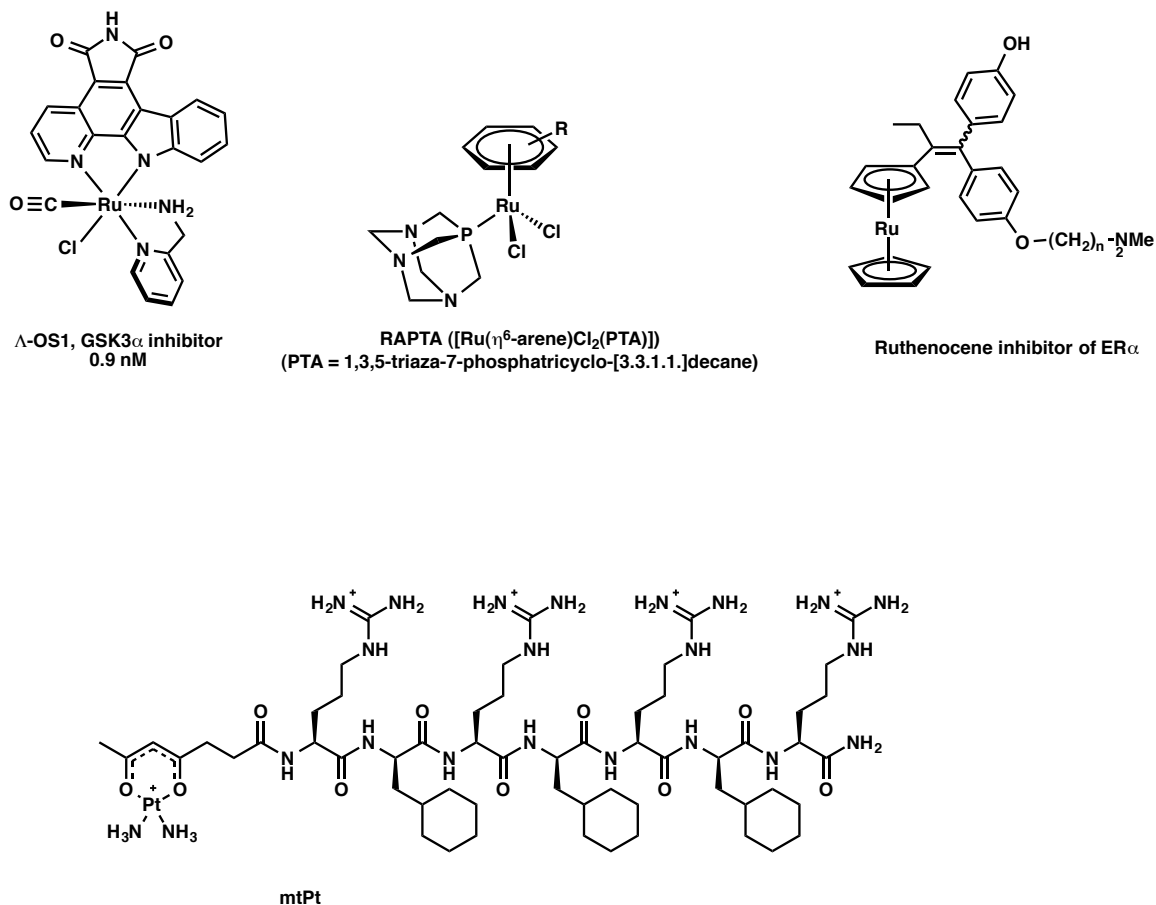


Figure 1.2 Chemical structures of targeted chemotherapeutics discussed in this Chapter: (top, left to right) The octasporine complex OS1, a potent inhibitor of the protein kinase GSK3a; General architecture of RAPTA cathepsin B inhibitors; Ruthenocene analogues of tamoxifen for the selective targeting of ERα; (bottom, left to right) The first generation rhodium metalloinsertor, $[\text{Rh}(\text{bpy})_2(\text{chrysi})]^{3+}$, selectively binds to mismatched and abasic sites in duplex DNA; Structure of mtPt, a cisplatin analogue designed to localize to the mitochondria.

1.3.1 Proteins as Targets

As an illustration, the high levels of mutagenesis in cancerous cells often lead to upregulation and overexpression of proteins, making them attractive candidates for targeting. Metal complexes, due to their modular nature and inherent chirality, are uniquely able to target selectively these chiral biomolecules. In particular, this approach has been applied toward the selective inhibition of kinase activity. Phosphorylation of proteins by kinases is a highly important regulatory activity. However, over-phosphorylation of proteins is common in many types of cancer.²⁸ In a recent study by Meggers et al., inert metal complexes, inspired by the natural product staurosporine and termed octasporines, were designed as highly selective kinase inhibitors (**Figure 1.2**).^{29,30} Six complexes were synthesized, all containing a ruthenium or iridium center and a bidentate pyridocarbazole ligand designed to bind the hinge region of the ATP-binding pocket of the kinase. However, the remaining ligands on each complex were designed to make up a unique set of hydrogen-bonding interactions with the glycine-rich loop of the ATP-binding pockets of six distinct kinases (**Figure 1.3**).²⁹ *In vivo* studies have revealed the anti-angiogenic properties of one of these types of compounds in zebrafish embryos, exemplifying their potential.³⁰

Whereas the previous example utilized the structural complexity of inert metal complexes, the reactive nature of certain metal centers can also be exploited in targeted therapy. Proteases play a crucial role in tumorigenesis by suppressing cell-death pathways and promoting cell-survival pathways.³¹ One such protease, cathepsin B, has been targeted by ruthenium arene RAPTA compounds (**Figure 1.2**).^{32,33} These compounds were found to inhibit cathepsin B protease activity and exhibited selective anti-metastatic

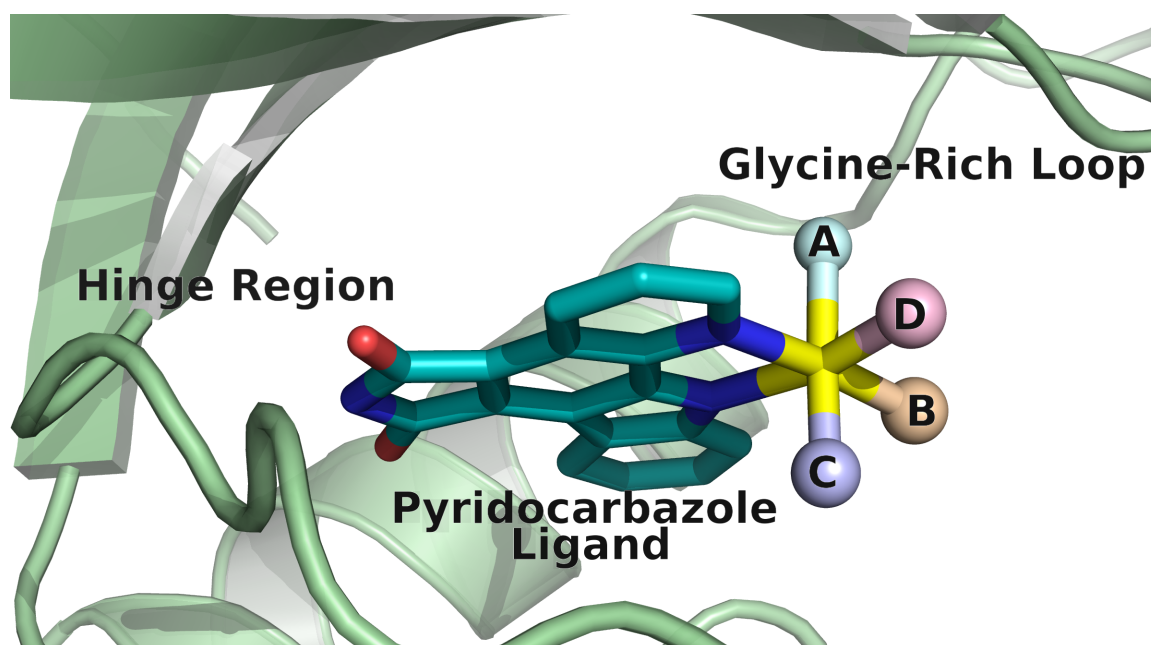


Figure 1.3 Design of Octasporine complexes as inhibitors of protein kinases (adapted from reference 32). The pyridocarbazole ligand, common to all complexes, binds to the hinge region (where the adenine portion of ATP binds) of the ATP-binding pocket. The remaining A, B, C, and D ligands make up a set of hydrogen-bonding interactions with the glycine-rich loop (where the ribose triphosphate portion of ATP binds) of the ATP binding pocket, each unique to a particular kinase.

activity *in vivo*.^{33,34} Estrogen receptors such as estrogen receptor α (ER α), which is over-expressed in several types of breast cancer, have also been the subject of targeted therapy studies.³⁵ Several organometallic analogues of tamoxifen, an antagonist of estrogen receptors, have been developed to selectively target ER α (Figure 1.2).^{36,37} These complexes have demonstrated cytotoxic activity selectively in ER α -positive breast cancer cell lines.³⁶

1.3.2 Organelles as Targets

In addition to protein targeting, the mitochondria can also serve as a valuable target for drug design. Mitochondria produce reactive oxygen species as a byproduct of metabolism, and they also play a crucial role in the regulation of cell death pathways.³⁸ Targeting mitochondria and mitochondrial DNA can induce apoptosis in tumorigenic cells, as was recently demonstrated by Lippard and Kelley.³⁹ They constructed a *cis*-platinum(II) complex tethered to a mitochondrial penetrating peptide, which contained alternating cationic and lipophilic residues to enhance mitochondrial uptake (**Figure 1.2**). This complex was shown to localize almost exclusively to mitochondria in several cancer cell lines. Moreover, the complex was able to induce apoptosis in cisplatin-resistant ovarian cancer cells by damaging mitochondrial DNA.

1.4 DNA as a Target: Noncovalent Binding

It has been established that DNA is the primary therapeutic target of cisplatin and its derivatives. The mechanism of action of classical platinum-based chemotherapeutics is the formation of covalent DNA adducts, followed by cellular processing of these lesions.⁴ The synthesis of new generations of classical therapeutics with enhanced DNA binding properties in order to increase cytotoxicity have been extensively explored. How-

ever, the design and synthesis of therapeutics that bind specific DNA lesions that are more prevalent in cancer cells than normal cells may represent a targeted strategy for new chemotherapy.

A major deviation from classical inorganic chemotherapeutics like *cis*-platinum is the development of metal complexes that do not form covalent crosslinks with DNA, but rather bind noncovalently and, therefore, reversibly. Here, the metal center remains substitutionally and oxidatively inert and instead acts as a scaffold for the ligands to interact with DNA. These complexes typically contain low spin, d^6 metal centers with octahedral geometry, such as Rh (III), Ru (II), Ir (III), Os (II), and Re (I), that are coordinatively saturated, usually with aromatic bidentate ligands.⁴⁰

The inert metal center anchors its ligands in chiral, three-dimensional geometries that can be modulated for specific interactions with DNA. In some of the earliest work on complexes of this nature, performed with tris(phenanthroline) complexes of ruthenium (II) and other metals, two distinct DNA binding modes were observed. One binding interaction was characterized by hydrophobic interactions between the ligands and the minor groove of DNA, as is the case for Λ -[Rh(phen)₃]²⁺ (phen = 1,10-phenanthroline).⁴¹ A well known groove binder is [Cu(phen)₂]²⁺,⁴² which can also cleave the DNA backbone upon binding in the presence of oxidants.⁴³

The other binding mode was identified as partial intercalation of one of the phenanthroline ligands into the DNA duplex from the major groove, resulting in a π -stacking interaction between the ligand and the flanking base pairs. The metallointercalative DNA binding mode can be observed with the Δ -enantiomer of [Rh(phen)₃]²⁺ but not with the groove-binding Λ -enantiomer, highlighting the significance of chirality in the binding of

octahedral metal complexes to DNA, itself a chiral molecule.⁴¹ Indeed, the right-handed B-form DNA can only accommodate intercalation from similarly right-handed Δ -enantiomers of octahedral metal complexes (**Figure 1.4**).⁴⁴

1.4.1 Metallointercalators

Metallointercalators, like their organic intercalator counterparts, unwind the DNA helix to π -stack between two consecutive base pairs. Metallointercalation is thus generally best achieved with planar, aromatic ligands that protrude away from the metal center, facilitating interactions with the base stack. Intercalating ligands phi (9,10-phenanthroline diimine) and dppz (dipyrido[3,2-*a*:2'.3'-*c*]phenazine) have been extensively studied by the Barton laboratory and others. In metallointercalators $[\text{Ru}(\text{bpy})_2(\text{phi})]^{2+}$ and $[\text{Ru}(\text{bpy})_2(\text{dppz})]^{2+}$, both intercalating ligands contain aromatic groups that extend away from the site of coordination to the metal center (**Figure 1.5**). These complexes also bind DNA from the major groove and are highly enantiospecific.⁴⁵

Metallointercalative binding has significant physical and chemical implications for the DNA to which it is bound. To accommodate the incoming intercalating ligand, the helical rise (i.e., the vertical distance between consecutive base pairs) doubles, and the major groove widens at the binding site.^{45,46} This lengthening of the duplex is accompanied by an increase in the viscosity of the DNA in solution.⁴⁷ Intercalation also enhances the thermodynamic stability of the duplex, increasing the melting temperature.⁴⁸ Interestingly, while metallointercalation induces local distortions to the duplex at the site of binding, the long-range structural effects are minimal. Unlike *cis*-platinum binding, metallointercalation does not bend the duplex, and the sugars and bases maintain their C_2' -endo and *anti* conformations, respectively.^{46,48}

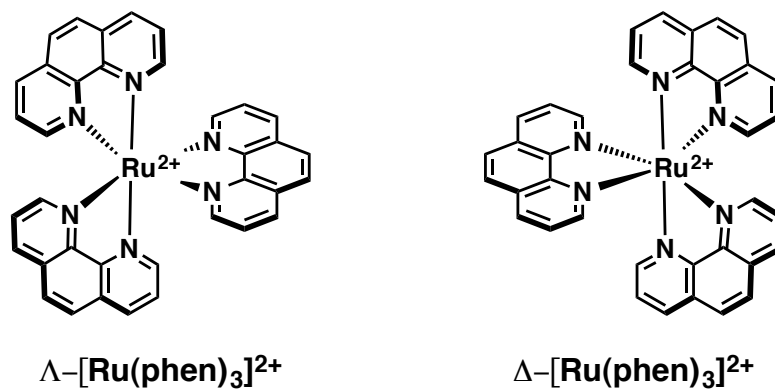


Figure 1.4 Chemical structures of octahedral ruthenium (II) tris(phenanthroline) complexes. Left: Λ -[Ru(phen)₃]²⁺, which interacts with DNA via minor groove binding interactions. Right: Δ -[Ru(phen)₃]²⁺, which interacts with DNA via partial intercalation of a phen (1,10-phenanthroline) ligand from the major groove.

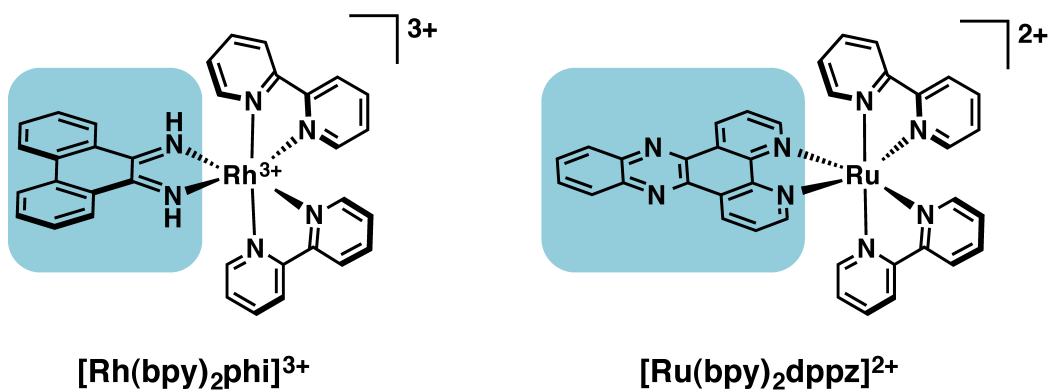


Figure 1.5 Chemical structures of Δ -[Rh(bpy)₂phi]³⁺ (left) and Δ -[Ru(bpy)₂dppz]²⁺ (right). Intercalating ligands phi (9,10-phenanthroline diimine) and dppz (dipyrido[3,2-*a*:2'.3'-*c*]phenazine) are highlighted in blue. These planar, aromatic ligands extend away from the metal center and π -stack between two adjacent base pairs in the DNA duplex, acting essentially as another base pair. [Rh(bpy)₂phi]³⁺ cleaves the DNA upon irradiation with UV light; [Ru(bpy)₂dppz]²⁺ is a DNA “light switch;” the complex is non-emissive in aqueous solvent but luminesces upon binding to DNA via intercalation. These complexes are also highly enantiospecific in their binding – the Λ -enantiomers do not readily bind to B-form DNA.

The applications of metallointercalation extend beyond altering the physical properties of DNA. Despite the substitutional inertness of the coordinatively saturated, low-spin heavy metal centers, the electronic configurations of these transition metals enable rich photochemistry and luminescence properties generally not afforded to organic intercalators. In one of the most well-studied examples of metallointercalation, the complex $[\text{Ru}(\text{bpy})_2\text{dppz}]^{2+}$ (bpy = 2,2'-bipyridine, **Figure 1.5**) exhibits solvatochromatic luminescence in organic solvents at ambient temperature, yet this luminescence is quenched in aqueous solution due to hydrogen bonding interactions between water and the phenazine nitrogen atoms of dppz. Upon intercalative binding to DNA, however, luminescence is restored as the π -stacking interactions within the duplex protect the ligand from solvation, thus becoming, famously, a “light switch” for DNA.⁴⁹

DNA light switch complexes of ruthenium and other metals have been extensively reported. Derivatives of $[\text{Ru}(\text{bpy})_2\text{dppz}]^{2+}$ have been developed wherein the luminescence properties are tuned via variation of the non-intercalating ancillary ligands – such as $[\text{Ru}(\text{phen})_2\text{dppz}]^{2+}$ and $[\text{Ru}(\text{DIP})_2\text{dppz}]^{2+}$ (DIP = 4,7-diphenyl-1,10-phenanthroline) – in addition to complexes containing altogether new intercalating ligands. The luminescence properties of DNA-binding transition metal complexes have been heavily investigated as potentially powerful diagnostic tools and imaging agents for cellular studies.⁵⁰⁻⁵³

In addition to robust luminescence, octahedral metallointercalators can also mediate photochemical reactions upon binding to DNA. Rhodium-based intercalators, such as $[\text{Rh}(\text{bpy})_2\text{phi}]^{3+}$ and $[\text{Rh}(\text{phen})_2\text{phi}]^{3+}$ (**Figure 1.6**), have been shown to induce single strand scission of the DNA backbone upon irradiation with short-wave ultraviolet (UV) light (313-325 nm).⁵⁴ Photoactivation of these complexes intercalated into

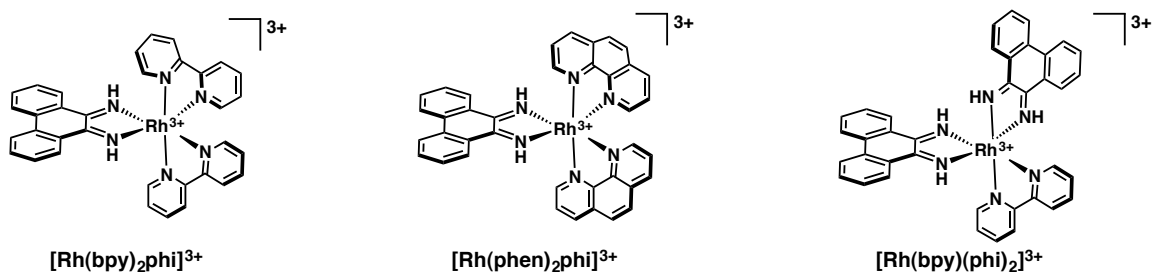


Figure 1.6 Rhodium (III) intercalators: Δ - $[\text{Rh}(\text{bpy})_2\text{phi}]^{3+}$ (left); Δ - $[\text{Rh}(\text{phen})_2\text{phi}]^{3+}$ (center); Δ - $[\text{Rh}(\text{phi})_2\text{bpy}]^{3+}$ (right). These complexes photocleave the DNA on one strand at the site of binding upon irradiation with UV-light.

DNA triggers the formation of a ligand-based radical that abstracts a hydrogen atom from the deoxyribose ring of a neighboring nucleotide.⁵⁵ It is the subsequent degradation of the sugar radical that prompts DNA cleavage at that site. For complexes intercalated from the major groove, it is proposed that this initial hydrogen atom abstraction occurs at the C2' of the adjacent sugar, and hydrogen migration to form the observable C3' radical occurs prior to degradation of the ribose ring.

The photochemistry of metallointercalators usefully enables facile visualization and quantification of DNA binding events by electrophoretic mobility shift assay (EMSA); the migratory differences of cleaved (i.e., complex bound) and non-cleaved (no complex bound) DNA can be observed with radiolabeled oligonucleotides on a denaturing polyacrylamide gel. This provides information regarding the site of binding as well as the amount of complex bound, allowing for the determination of equilibrium binding constants. Potential therapeutic applications of photocleaving intercalator complexes have been explored, as light-induced DNA strand scission is often accompanied by the generation of reactive oxygen species (ROS), which are toxic to the cell.⁵⁶ Photoactive rhodium intercalators have also been employed as redox probes to monitor the migration of electrons and holes through the DNA π -stack – a remarkable phenomenon known as DNA charge transport.⁵⁷

1.4.2 Metallointercalators for Selective DNA Recognition

Overall, metallointercalators are a highly diverse class of inorganic complexes with versatile applications for DNA recognition. However, the nature of the metallointercalative binding mode is by definition nonspecific: the intercalating ligand is accepted into the base stack, acting essentially as a new base pair. This interaction can occur any-

where in the DNA sequence with little discrimination, thereby limiting the application of metallointercalators for targeted therapy.

Efforts to tune the specificity of metallointercalators have exploited the three-dimensional architecture of octahedral metal complexes as well as their modular synthesis. By exchanging ligand sets, it is possible to alter the shape of the complex and, consequently, the nature of its interactions with DNA. The notion of shape-selective DNA recognition stems in part from the highly enantiospecific nature of metallointercalation. Intercalation of a protruding aromatic ligand, such as dppz or phi, into the base stack situates the metal center with its non-intercalating ancillary ligands in the major groove. Thus, the source of the enantiospecificity in intercalative binding stems from steric interactions between the ancillary ligands and the sugar-phosphate backbone of DNA. When the Δ -enantiomer of a metallointercalator binds DNA, the ancillary ligands fit in the major groove, but substantial steric clashing would be encountered if the Λ -enantiomer were bound. As a result, increasing the size of the ancillary ligands can further enhance chiral discrimination.⁴⁴ The geometry and symmetry of metallointercalators, too, can also be advantageous for selective DNA recognition. Bis(heteroleptic) intercalator complexes such as $[\text{Rh}(\text{phen})_2(\text{phi})]^{3+}$ are generally referred to as “octahedral” but in actuality possess C_2 symmetry, affording a propeller twist to these complexes that can be functionalized to preferentially bind specific nucleotide patterns in DNA.⁴⁶

An intricate example of selective recognition can be found in the aforementioned Δ - α - $[\text{Rh}((R,R)\text{-Me}_2\text{trien})(\text{phi})]^{3+}$ complex, shown in **Figure 1.7**. This photocleavage agent was rationally designed to bind and photocleave specifically at 5'-TGCA-3' sites. The selectivity arises from hydrogen bonding contacts between the axial ammine ligands

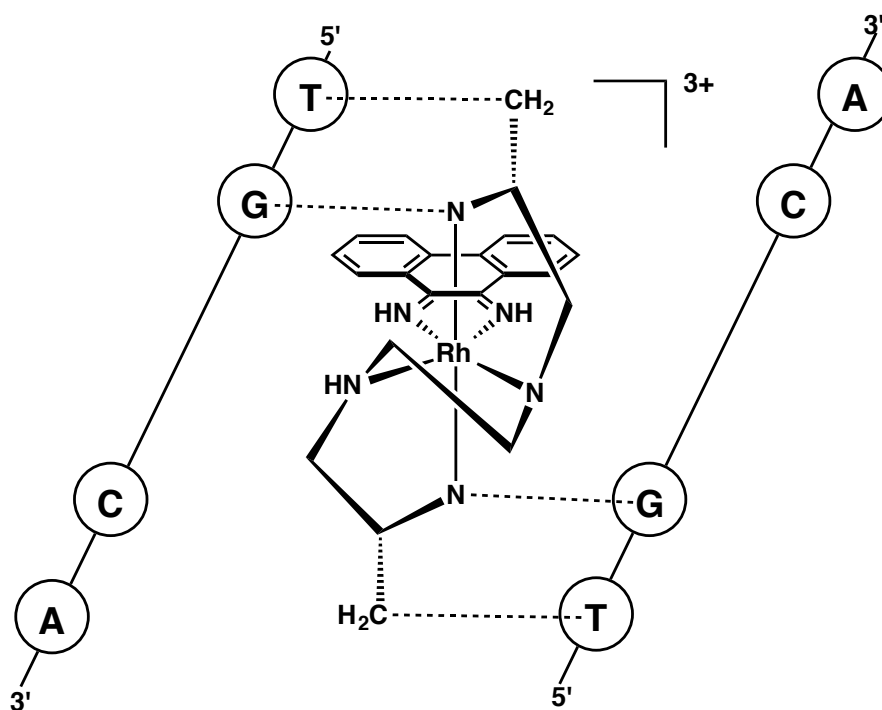


Figure 1.7 Structure of $\Delta\text{-}\alpha\text{-}[\text{Rh}[(\text{R},\text{R})\text{-Me}_2\text{trien}]\text{phi}]^{3+}$ and schematic illustration of the complex binding to its 5'-TGCA-3' recognition sequence. Intercalation of the phi ligand occurs between the GC base pairs. The sequence specificity arises from hydrogen-bonding interactions between the axial NH_2 groups of the ligand and the O_6 -position of the guanines, as well as methyl-methyl interactions between the ligand methyl groups and the methyl groups of the thymine residues.

and the *O6* position of the guanine residues as well as hydrophobic interactions between the methyl groups of the trien ligands and the thymine residues. This complex intercalates with such extraordinary sequence specificity that the first high-resolution crystal structure of a metallointercalator bound to DNA could finally be obtained, revealing a detailed picture of the metallointercalative binding mode.⁵⁸

Many other examples of sequence- and shape-selective metallointercalator complexes have been developed. However, even the most selective complexes have few applications in targeted therapy, as their small, ubiquitous recognition sequences provide little discrimination between healthy and cancerous cells. Additionally, the minimal, localized helical distortions incurred by intercalation often do not create lesions that are critical to cell survival, and thus are not cytotoxic in the absence of UV-damage or oxidative stress. The ultimate goal, then, is the development of metal complexes that can target sites within the DNA that are specific to cancerous cells but are not found in healthy cells.

1.4.3 Metalloinsertors

A major advancement in the development of metal complexes that could specifically target cancerous DNA defects has been the design of octahedral rhodium (III) complexes that bind selectively to base pair mismatches. This class of molecules bears resemblance to rhodium (III) metallointercalators, except the intercalating “phi” ligand – which, at 9.2 Å wide, nonspecifically intercalates into DNA unless guided by ancillary ligands toward specific binding sites – is replaced with a sterically expanded derivative, chrysi (5,6-chrysenequinone, **Figure 1.8**).⁵⁹ Possessing an additional fused benzene ring, the 11.3 Å-wide chrysi ligand is too large to intercalate, as a DNA base pair is only 10.8

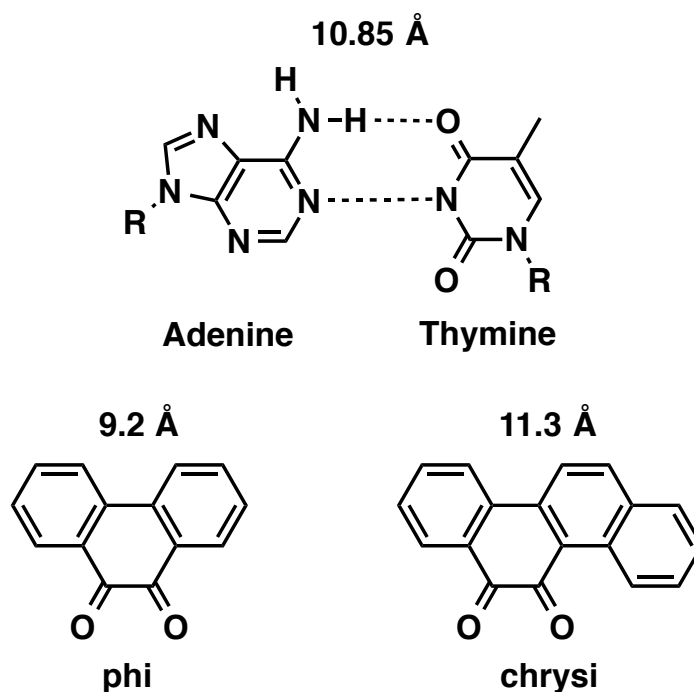


Figure 1.8 Comparison of the width of intercalating ligand phi (9.2 Å across) and inserting ligand chrysi (5,6-chrysenequinone; 11.3 Å across). A standard Watson-Crick base pair is 10.85 Å across; thus, phi is narrow enough to intercalate in the base stack. The chrysi ligand, expanded by an additional fused benzene ring, is too wide for nonspecific intercalation. Thus, this ligand only binds DNA at thermodynamically destabilized sites, such as mismatches, wherein the destabilized base pairs can be ejected from the duplex, leaving enough room for the chrysi ligand to insert into the base stack.

Å across; thus, all nonspecific binding is eliminated. In contrast, single base lesions such as mismatches or abasic sites are thermodynamically destabilized compared to canonical Watson-Crick base pairs, due to imperfect hydrogen bonding between the mismatched bases as well as perturbations in the π -stack. Overall, mismatches in DNA are approximately 3-5 kcal/mol more destabilized than well-matched base pairs, resulting in a dynamic site that is stabilized by the intrusion of the chrysi ligand.^{60,61} In this new binding mode, termed *metalloinsertion*, the chrysi ligand displaces both mismatched base pairs from the helix, inserting fully into the intervening space.^{62,63} Stacking interactions between the expansive chrysi and the flanking base pairs recuperate the energy cost of extruding the mismatch. This metalloinsertive binding mode, which occurs from the minor groove, was predicted by L. S. Lerman in 1961,⁶⁴ nearly 50 years before it would be confirmed crystallographically for the first time by the Barton laboratory.⁶³

The first-generation metalloinsertor complex, $[\text{Rh}(\text{bpy})_2\text{chrysi}]^{3+}$, was synthesized in the Barton laboratory and characterized by *in vitro* DNA binding experiments.^{59,65} Like its rhodium (III) intercalator counterparts, $[\text{Rh}(\text{bpy})_2\text{chrysi}]^{3+}$ induces single-strand scission at the ribose adjacent to the site of binding upon irradiation (although in this case, hydrogen abstraction occurs at the C1' position of the sugar, due to the positioning of the complex in the minor groove). This photocleavage was shown to occur exclusively at mismatched sites, and the equilibrium binding constants for mismatch recognition correlated directly to the thermodynamic stability of the mismatches themselves. That is, the stability of the base pairs – $\text{C}\cdot\text{G} > \text{A}\cdot\text{T} \gg \text{G}\cdot\text{G} \sim \text{G}\cdot\text{T} \sim \text{A}\cdot\text{G} > \text{T}\cdot\text{T} \sim \text{A}\cdot\text{A} > \text{C}\cdot\text{T} \sim \text{A}\cdot\text{C} > \text{C}\cdot\text{C}$ – corresponds to the ease of recognition by $[\text{Rh}(\text{bpy})_2\text{chrysi}]^{3+}$, with cytosine-containing mismatches being the most destabilized and thus the most easily bound.^{66,67}

For instance, the binding affinity of $[\text{Rh}(\text{bpy})_2\text{chrysi}]^{3+}$ to a CC mismatch is $3 \times 10^7 \text{ M}^{-1}$, compared to $2.9 \times 10^5 \text{ M}^{-1}$ for an AA mismatch.⁶⁶ Guanine-containing mismatches, in contrast, are significantly more stable, and consequently are not recognized by metalloinsertors. Overall, metalloinsertors can bind 80% of all mismatches, regardless of the surrounding sequence context.⁶⁸

The extraordinary selectivity of these complexes for DNA mismatches was revealed through photocleavage experiments with a 2725 base pair linearized plasmid containing a single CC mismatch. Upon irradiation with $[\text{Rh}(\text{bpy})_2\text{chrysi}]^{3+}$, photocleavage was found to occur only at this site, with no evidence of binding in the well-matched control plasmid, corresponding to 1000 fold selectivity for mismatches over Watson-Crick base pairs. The first-generation metalloinsertors also display remarkable enantiospecificity, with only the right-handed Δ - $[\text{Rh}(\text{bpy})_2\text{chrysi}]^{3+}$ and Δ - $[\text{Rh}(\text{bpy})_2\text{phzi}]^{3+}$ (phzi = benzo[*a*]phenazine-5,6-dione) enantiomers (**Figure 1.9**) capable of recognizing mismatches in B-DNA.⁶⁶

1.4.4 Metalloinsertors as Targeted Chemotherapeutics

The metalloinsertion binding mode was structurally characterized by co-crystallization of $[\text{Rh}(\text{bpy})_2\text{chrysi}]^{3+}$ to palindromic DNA duplexes containing CA and AA mismatches, revealing the extrusion of the mismatched base pairs from the π -stack and the insertion of the chrysi ligand from the minor groove (**Figure 1.10**).^{63,69} Additionally, crystal structures of the intercalating DNA light-switch complex $[\text{Ru}(\text{bpy})_2\text{dppz}]^{2+}$ revealed a similar binding mode in the presence of mismatched DNA: the dppz ligand, too, was capable of ejecting mismatched base pairs in an insertive manner, albeit without the selectivity afforded by the expanded chrysi and phzi ligands.⁷⁰ These structural char-

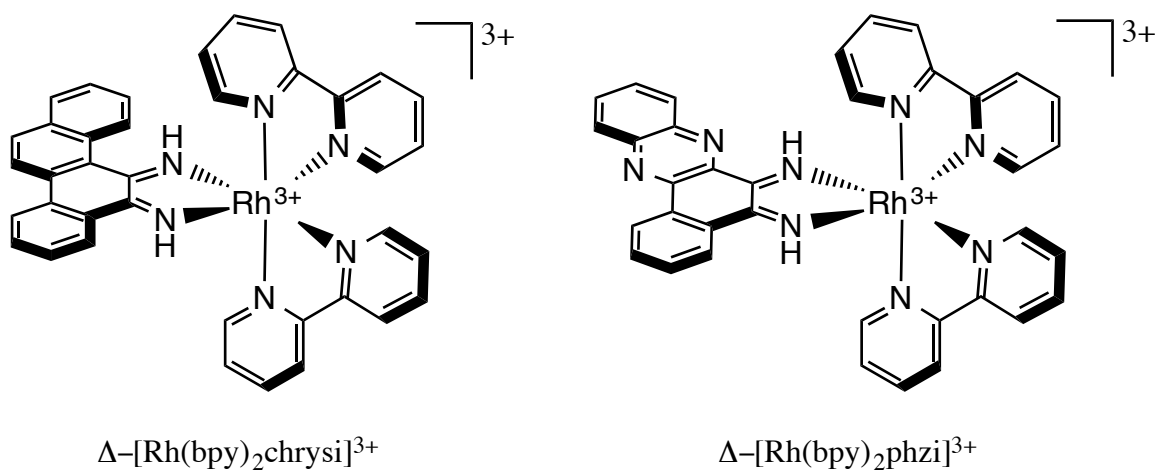


Figure 1.9 Chemical structures of Δ -[Rh(bpy)₂chrysi]³⁺ (left) and Δ -[Rh(bpy)₂phzi]³⁺ (right), the first- and second-generation metalloinsertor complexes, respectively. The sterically expansive inserting ligands, chrysi (5,6-chrysenequinone diimine) and phzi (benzo[*a*]phenazine-5,6-diimine) target thermodynamically destabilized base pair mismatches with over 1000-fold specificity.

acterizations are a testament to the generality of metalloinsertion. Additionally, although metalloinsertion incurs minimal distortions to the duplex with no increase in helical pitch, the ejection of the mismatched bases results in a large lesion that is hypothesized to have the potential to be recognized *in vivo*.

Mismatches in genomic DNA arise naturally as a consequence of replication, but if left uncorrected can lead to mutations.^{71,72} The mismatch repair (MMR) pathway serves as a checkpoint to increase the fidelity of DNA replication ~1000 fold.⁷³ Importantly, deficiencies in the mismatch repair machinery have been associated with several types of cancer, as well, notably, as increased resistance to classical chemotherapeutics such as cisplatin.⁷⁴ Therefore, the development of a targeted therapy for MMR- deficient cancers would be invaluable in the clinic. Due to the unique DNA mismatch-binding properties of rhodium metalloinsertors, we sought to explore their biological properties in MMR-deficient cells. The compounds were initially found to inhibit growth in MMR-deficient colorectal cancer cells over MMR-proficient cells, as measured by antibody assays for DNA synthesis.^{75,76} In a follow-up study, it was discovered that metalloinsertors with accelerated uptake also exhibited preferential cytotoxicity towards MMR-deficient cells (**Figure 1.10**).⁷⁷ Additionally, these complexes were discovered to induce a necrotic mechanism of cell death, rather than the caspase-dependent, programmed apoptotic mode induced by *cis*-platinum therapeutics.

The synthesis of large families of second- and third-generation metalloinsertors enabled the elucidation of structure-activity relationships critical for optimizing biological activity. It had previously been shown that the size of the ancillary ligands directly correlated to the mismatch binding affinity of metalloinsertors; small ligands, such as

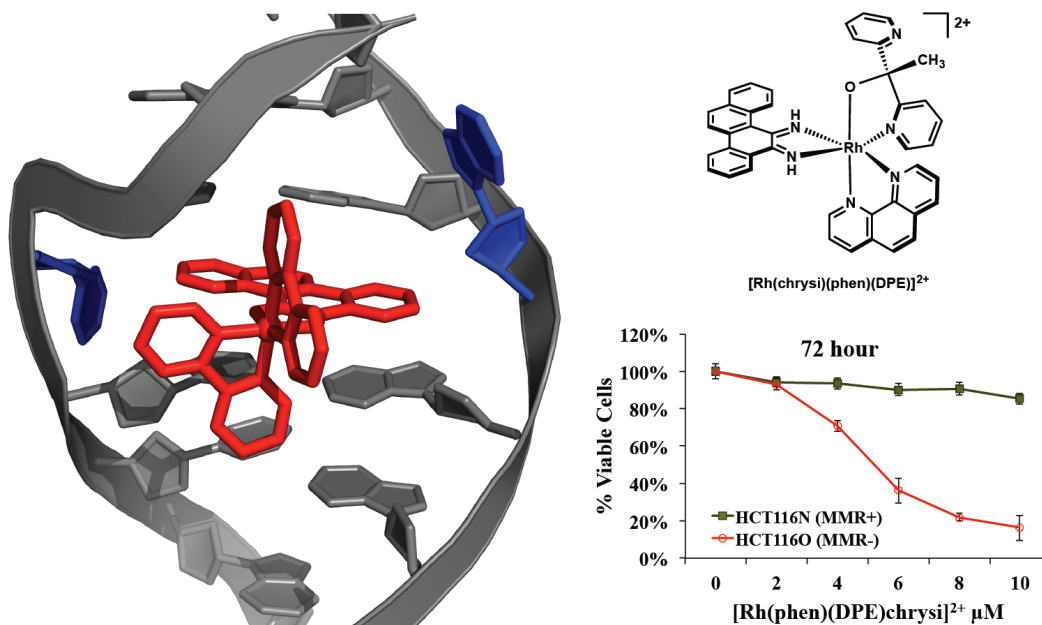


Figure 1.10 (Left) Crystal structure of $[\text{Rh}(\text{bpy})_2(\text{chrysi})]^{3+}$, the first generation metal-loinsertor, bound to an AC mismatch in duplex DNA. (Right, top) Chemical structure of $[\text{Rh}(\text{chrysi})(\text{phen})(\text{DPE})]^{2+}$, a later generation metalloinsertor with enhanced selectivity and potency. (Right, bottom) Cell-selective cytotoxicity of $[\text{Rh}(\text{chrysi})(\text{phen})(\text{DPE})]^{2+}$, the complex selectively kills MMR-deficient (red) cells over MMR-proficient (green) cells.

ammines, allow for tighter binding due to minimal steric interactions with the sugar-phosphate backbone, compared to bulky ligands like DIP, which confer critically weak binding affinities (**Figure 1.11**). It was found that the binding affinity for a mismatch translated to enhanced differential activity – that is, preferential antiproliferative activity in MMR-deficient cells.⁷⁶ Most recently, a structure-function study was conducted by altering the lipophilicities of the non-inserting ligands.^{78,79} This investigation resulted in the synthesis of a family of mismatch-binding complexes with similar binding affinities and selectivities for DNA mismatches, yet drastically different selectivities for MMR-deficient cells. It was discovered that more lipophilic complexes did not exhibit the unique cell-selective activities for which metalloinsertors are distinguished. However, complexes with more hydrophilic ancillary ligands were highly selective for the MMR-deficient cells over MMR-proficient cells. It was discovered that nuclear uptake of all metalloinsertors studied was sufficient for mismatch binding to genomic DNA. However, significant mitochondrial uptake led to an abolishment of their selective targeting of MMR-deficient cells. Most notably, simply substituting a hydroxyl group for a methyl group results in dramatic changes in cell-selective activity due to drastic changes in the subcellular localization (**Figure 1.12**).⁷⁹ This study supports the notion that the unique cell-selective activities of these compounds rises from targeting of mismatches in genomic DNA. In an effort to more directly relate the biological activity of rhodium metalloinsertors to the MMR-deficiency phenotype, our laboratory has now embarked on studies to validate the biological efficacy of these compounds.

All of the cell assay experiments characterizing the *in cellulo* effects of rhodium metalloinsertors had been undertaken on the isogenic cell lines HCT116N and HCT116O.

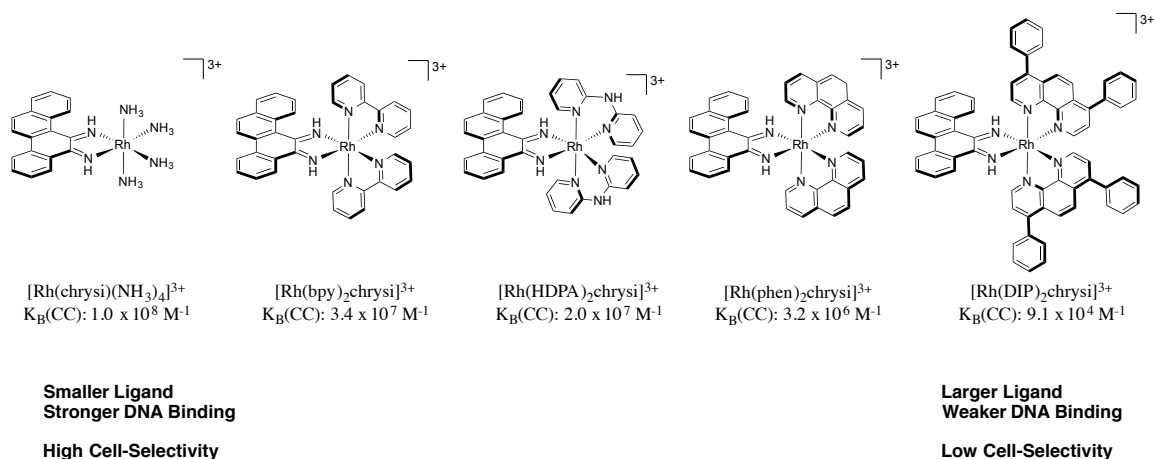


Figure 1.11 Effects of the non-inserting ancillary ligands on the biological activity of rhodium metalloinsertors. Increasing the size of the ancillary ligands imparts steric clashing with the sugar-phosphate backbone upon DNA mismatch recognition; thus, equilibrium binding constants are weaker for complexes with large ligands, as is the case for $[\text{Rh}(\text{DIP})_2\text{chrysi}]^{3+}$. In contrast, complexes with small ligands display tighter binding to DNA mismatches, as is the case with $[\text{Rh}(\text{chrysi})(\text{NH}_3)_3]^{3+}$, due to the lack of steric interference. In a family of five complexes, the *in vitro* DNA binding affinities correlated directly to the differential antiproliferative activity – that is, the preferential inhibition of DNA synthesis in the MMR-deficient HCT116O colorectal cancer cells over the MMR-proficient HCT116N cell line.

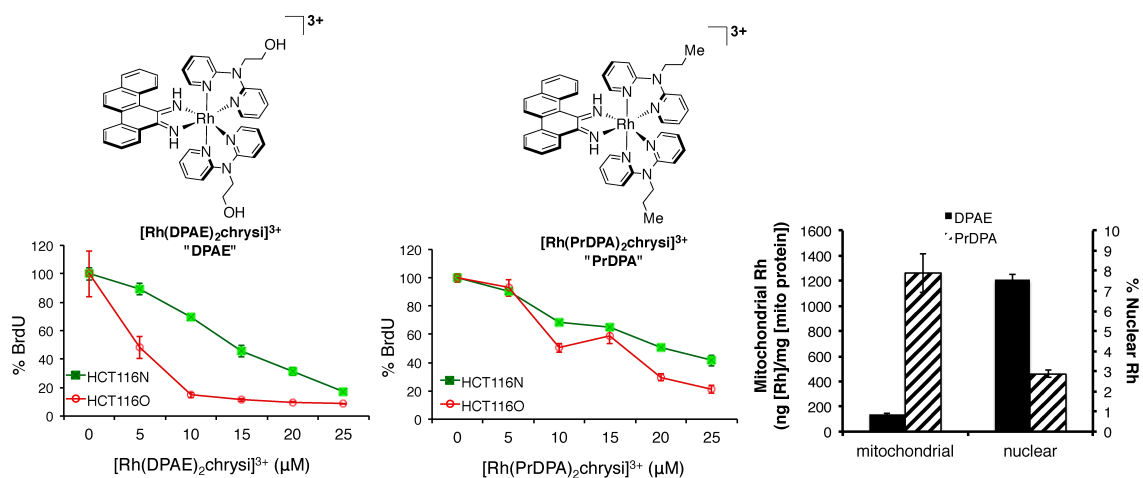


Figure 1.12 Inhibitory effects of $[\text{Rh}(\text{DPAE})_2\text{chrysi}]^{3+}$ (bottom, left) and $[\text{Rh}(\text{PrDPA})_2\text{chrysi}]^{3+}$ (bottom, center) on cellular proliferation in MMR-deficient HCT116O (red) and MMR-proficient HCT116N (green) cells as a function of BrdU incorporation during DNA synthesis (adapted from reference 79). Percent BrdU incorporation is normalized to that of untreated cells. (Bottom, right) Subcellular localization of $[\text{Rh}(\text{DPAE})_2\text{chrysi}]^{3+}$ (black) and $[\text{Rh}(\text{PrDPA})_2\text{chrysi}]^{3+}$ (hashed). Mitochondrial rhodium content (left axis) has been normalized to mitochondrial protein content, and nuclear rhodium content (right axis) is expressed as the percentage of cellular rhodium in the nucleus.

The HCT116 parent cell line is a human colorectal carcinoma line deficient in the *hMLH1* gene. This gene encodes for part of the mismatch repair (MMR) machinery; consequently this cell line is MMR-deficient. The HCT116N cell line has been transfected with human chromosome 3 (ch3), which restores MMR proficiency, while the HCT116O cell line has been transfected with human chromosome 2 (ch2), leaving it MMR-deficient.⁸⁰ In this model system, however, the MMR-proficient cells and MMR-deficient cells are generated as different clones, and are distinct from the parental cell line. These differences can result in changes in chromosome stability or gene expression that are not solely due to MMR deficiency. To this end, we engineered NCI-H23 lung adenocarcinoma cells that contain a doxycycline-inducible short hairpin RNA (shRNA) that suppresses the expression of the mismatch repair gene *MLH1*. This provides an isogenic cell line system that can be used to directly compare MMR-proficient and MMR-deficient cells.⁸¹

It was found that these *MLH1*-deficient cells, which are more resistant to the DNA damaging agents doxorubicin, cisplatin, and etoposide, are indeed more sensitive to rhodium metalloinsertors (**Figure 1.13**).⁸¹ These results further validate the biological activity of rhodium metalloinsertors, as they have now been shown to exhibit selective biological effects across multiple assays and in different systems for comparing MMR deficiency to proficiency. Clearly, the strategy of targeting a specific lesion in DNA is a promising alternative to the classical approach.

1.5 Expanding the Reactivity of Metalloinsertors: Bifunctional Conjugates

Rhodium metalloinsertors are a robust class of complexes that offer a promising alternative for targeting MMR-deficient cancers and circumventing resistance. New generations of metalloinsertors, derived from the first-generation $[\text{Rh}(\text{bpy})_2\text{chrysi}]^{3+}$ and

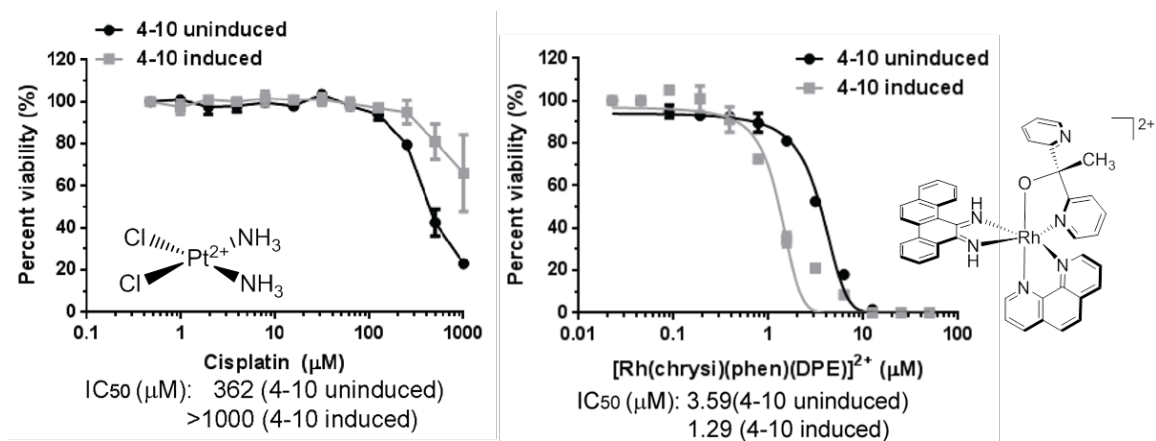


Figure 1.13 NCI-H23 subclones that were uninduced or induced for MLH1 shRNA were treated with either cisplatin (left) or the rhodium metalloinsertor $[\text{Rh}(\text{chrysi})(\text{phen})(\text{DPE})]^{2+}$ (right) (adapted from reference 81). Cells were treated at concentrations indicated, and cell viability assessed after 4 days using a Cell Titer-Glo assay. IC_{50} values are shown below the plots.

$[\text{Rh}(\text{bpy})_2\text{phzi}]^{3+}$ have exhibited increased potency surpassing that of cisplatin, while still maintaining selective targeting to MMR-deficiency.^{78,82} While these compounds are currently being explored as chemotherapeutic agents, they also hold promise as potential adjuvants that could confer their unique selectivity onto other therapeutic cargo.

Several bifunctional metalloinsertor conjugates have been developed for the targeting of therapeutic agents towards mismatched DNA, whereas in their native form they would interact with DNA in a nonspecific manner. In general, metalloinsertor conjugates are constructed as trisheteroleptic (three unique bidentate ligands) complexes, wherein one ancillary ligand is functionalized with the secondary subunit. The metalloinsertor subunit, then, acts as a directing agent that taxis its cargo preferentially towards mismatched sites in DNA.

1.5.1 Metalloinsertor-Alkylator Conjugate

The first bifunctional metalloinsertor conjugate designed in the Barton laboratory consisted of a $[\text{Rh}(\text{chrysi})(\text{phen})(\text{bpy}')]^{3+}$ subunit tethered to an aniline mustard, where bpy' is a 2,2'-bipyridine ligand modified with an amino-alkane tether (**Figure 1.14**). The nitrogen mustard melphalan, which forms covalent adducts with DNA at 5'-GNC-3' sites, was attached to the metalloinsertor via amide bond formation. The complex displayed a bifunctional binding mode involving both metalloinsertion of the rhodium-chrysi moiety at the mismatched site as well as the covalent alkylation of DNA by the melphalan subunit. Additionally, a seven-fold increase in alkylation of mismatched DNA was observed for the conjugate compared to well-matched binding, indicative of metalloinsertor-directed targeting. Furthermore, DNA alkylation proceeds more effectively and with increased site-specificity for the conjugate than with melphalan alone. Remarkably,

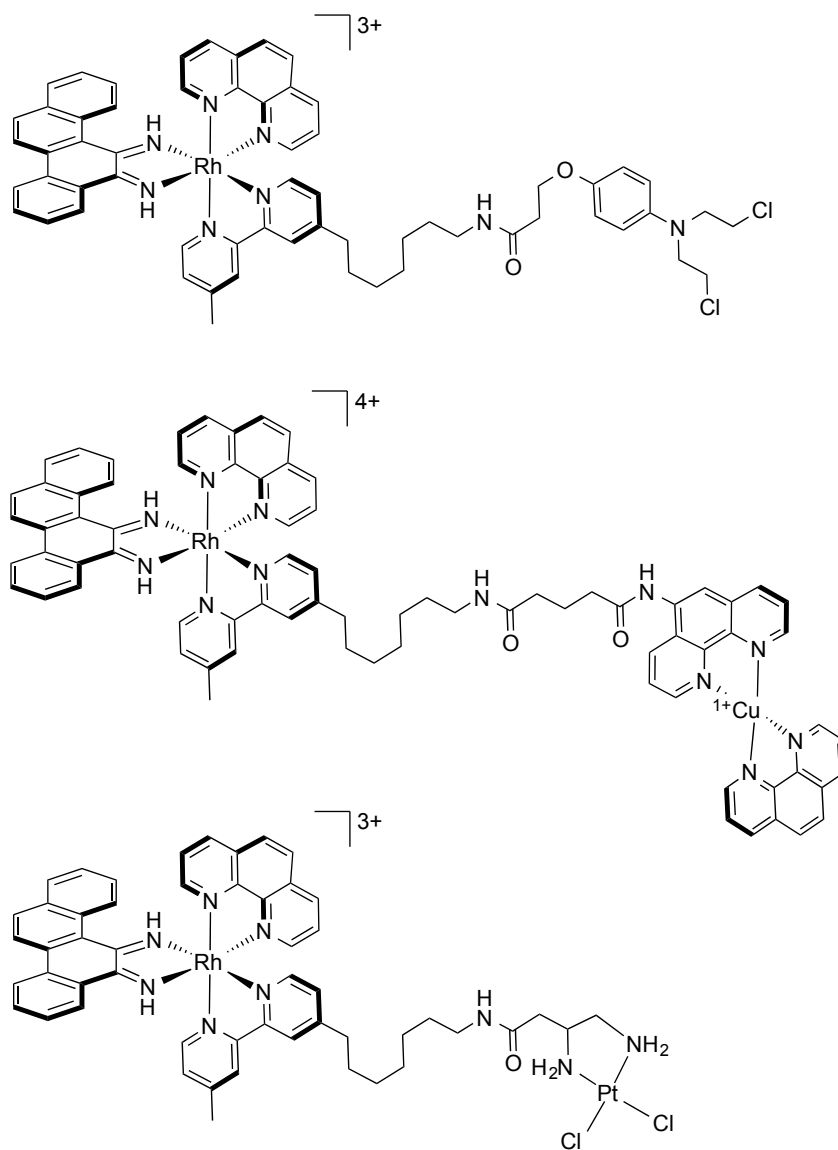


Figure 1.14 Chemical structures of bifunctional, mismatch-specific metalloinsertor conjugates: a metalloinsertor-nitrogen mustard conjugate for mismatch-directed alkylation of DNA (top); a bimetallic Rh(III)-Cu(I) conjugate, which displays selective cleavage of mismatched DNA in the absence of irradiation (middle); and a bimetallic Rh(III)-Pt(II) conjugate, which displays preferential platination of guanine residues on mismatched DNA duplexes (bottom).

the two distinct binding interactions are largely independent of one another, in that alkylation of DNA neither inhibits nor enhances the mismatch binding ability of the metalloinsertor group.⁸³

1.5.2 Metalloinsertor Conjugate for DNA Cleavage

A second example of mismatch-directed conjugate design involves the attachment of the DNA cleavage agent $[\text{Cu}(\text{phen})_2]^{2+}$ to a metalloinsertor (**Figure 1.14**). Again, the $[\text{Rh}(\text{chrysi})(\text{phen})(\text{bpy}')]^{3+}$ scaffold is employed. Here, the rhodium directs copper-induced cleavage of the DNA preferentially towards mismatched DNA. Interestingly, the rhodium induces this potentiating effect even when the two complexes are added as separate subunits. DNA cleavage is enhanced possibly due to the slight opening of the minor groove as a result of metalloinsertion. The therapeutic advantage of this conjugate is that DNA cleavage can be induced near mismatched sites in the absence of UV irradiation, which causes nonspecific damage to the genome.⁸⁴

1.5.3 Metalloinsertor-Cisplatin Conjugate

In recent years, many new strategies in inorganic drug design have been developed for both classical and targeted therapies. Nevertheless, the traditional *cis*-platinum drugs remain the only transition metal complexes approved for therapeutic use worldwide, despite their limitations. Due to the clinical significance of platinum, strategies for tuning its selectivity toward specific lesions in DNA would be invaluable in mitigating both cisplatin resistance as well as side effects arising from off-target toxicity.

A metalloinsertor functionalized with a cisplatin derivative was constructed in an analogous manner to the previous conjugates (**Figure 1.14**). Instead of two monodentate ammine ligands, a bidentate ethylenediamine functionalized with a carboxyl group was

employed for ease of synthesis. Again, the conjugate was shown to successfully target its cargo to mismatched DNA, where the platinum moiety forms both inter- and intrastrand crosslinks with duplex DNA at guanine residues. However, this preferential binding is highly dependent on the presence and location of a d(GpG) site (the preferred binding site of cisplatin); if there is no d(GpG) site, or if it is inaccessible to the platinum center due to limitations in the length and flexibility of the alkyl tether, then minimal platination occurs. Likewise, there was no preference for mismatched DNA in these scenarios. In order to achieve selective platination of mismatched DNA, a d(GpG) site must be present approximately nine base pairs away from the mismatched site, where the six-carbon alkyl tether most favors interactions between the platinum center and the DNA.⁸⁵ Unsurprisingly, this limitation reduces the applications of the conjugate in a biological system; indeed, when characterized in the isogenic HCT116N and HCT116O cell lines, the conjugate displayed no preferential antiproliferative activity in the MMR-deficient line, and in fact exhibited a small preference for the MMR-proficient HCT116N cells.⁸⁶

1.5.4 Metalloinsertors Conjugated to Cell-Penetrating Peptides

The previous examples of metalloinsertor conjugates demonstrate the ability of these complexes to confer their mismatch recognition capabilities onto other chemotherapeutic agents in their interactions with DNA. But some conjugates were designed with the purpose of enhancing the activity of metalloinsertors themselves. One notable example is the development of a rhodium metalloinsertor complex outfitted with a cell-penetrating peptide for enhanced cellular uptake. Highly charged peptide sequences, such as octaarginine tags, facilitate cellular transport of cargo through endocytosis.⁸⁷ When conjugated with a metalloinsertor complex, cellular uptake of rhodium was greatly en-

hanced compared to the typical passive diffusion uptake mechanism exhibited by metal complexes alone (**Figure 1.15**).⁸⁸ The goal of this project was to increase the potency of metalloinsertors through increasing the intracellular concentration of rhodium. However, while the conjugate was able to successfully increase cellular rhodium accumulation with the attachment of a cell-penetrating peptide, the high positive charge of the complex resulted in significant nonspecific, electrostatically-driven DNA binding.

1.5.5 Outlook for Bifunctional Metalloinsertor Conjugates

The current repertoire of bifunctional conjugates comprises a diverse and chemically complex family of metalloinsertors. In many ways, they have been successful in exhibiting dual functionality in their DNA binding behavior and unique chemical reactivities *in vitro*. In a biological context, however, these complexes have critically fallen short in their ability to selectively target MMR-deficiency like their monomeric counterparts. Furthermore, the development and biological characterization of new generations of rhodium metalloinsertors have revealed that cellular uptake, nuclear localization, and increased cell-selective potency could be achieved more simply by altering the chemical environment of the ancillary ligands.^{78,79,82} Most recently, it was found that a new family of rhodium metalloinsertor complexes bearing ligands that coordinate through a Rh—O bond (**Figure 1.16**) exhibit unprecedented selectivity and potency in MMR-deficient cells, with IC₅₀ values in the pharmaceutically significant 200-300 nM range. Remarkably, it was this simple Rh—O coordination that critically altered aspects of the complex, such as the pKa and planarity of the chrysi inserting ligand, leading to its enhanced biological activity and even enabling mismatch recognition by the formerly inactive Λ -enantiomers.⁸²

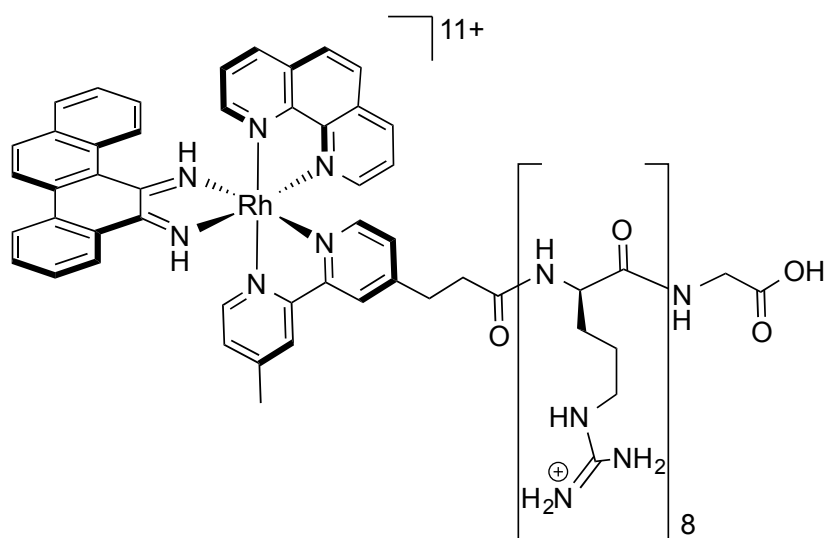


Figure 1.15 Structure of a metalloinsertor-peptide conjugate. A Rh(III) metalloinsertor complex was functionalized with an octaarginine cell-penetrating peptide. The peptide affords enhanced cellular and nuclear uptake of the complex while still enabling mismatch recognition by the rhodium subunit; however, nonspecific DNA binding is increased due to electrostatic interactions arising from the high positive charge of the peptide.

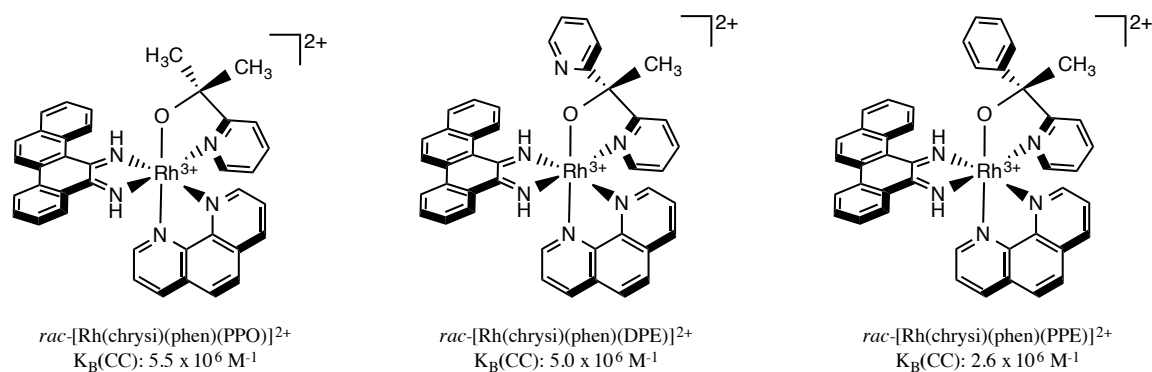


Figure 1.16 Chemical structures and binding affinities for a CC mismatch of a new family of metalloinsertor complexes bearing an unusual Rh—O ligand coordination: $[\text{Rh}(\text{chrysi})(\text{phen})(\text{PPO})]^{2+}$ (left, PPO = 1-methyl-1-(pyrid-2-yl)ethanol); $[\text{Rh}(\text{chrysi})(\text{phen})(\text{DPE})]^{2+}$ (center, DPE = 2,2'-pyridylethanol); and $[\text{Rh}(\text{chrysi})(\text{phen})(\text{PPE})]^{2+}$ (right, PPE = 1-phenyl-1-(pyrid-2-yl)ethanol). This new class of ligands forms an *N,O*-chelate, resulting in enhanced potency and selectivity, as well as a potentially new metalloinsertive binding mode that can accommodate both Δ - and Λ -enantiomers in the minor groove.

Given these recent discoveries, it may seem as though there is no longer a place for metalloinsertor conjugates in targeted therapy; metalloinsertors function magnificently on their own. And yet, the continued enhancement of metalloinsertor efficacy now more than ever enables their development not simply as chemotherapeutics in and of themselves, but also as potentially useful tools in targeted adjuvant therapy. Even common chemotherapeutics such as cisplatin are currently administered in conjunction with one or more additional drugs, each functioning separately but often synergistically within a cell.⁸⁹ The ability to functionalize metalloinsertors as cell-selective delivery agents for additional therapeutically useful cargo would be invaluable in the clinic. Additionally, as our rhodium complexes progress beyond tissue culture and into a more clinical setting, it may become necessary to modify these metalloinsertors with cell- and tissue-targeting functionalities, such as peptides or antibodies, to control biodistribution *in vivo*. It is difficult to predict how these complexes will fare in multicellular organisms and complex tumor microenvironments, just as the anticancer properties (and consequent adverse effects) of cisplatin could not have been foretold prior to their discovery. The continued modulation of both mono- and bifunctional metalloinsertors ensures a diverse repertoire of potentially powerful therapeutic tools.

1.6 Conclusions

Targeted chemotherapy holds the potential to combat the severe side effects and acquired resistance associated with classical chemotherapeutics such as cisplatin. Many years of study have focused on achieving high potency for metal complex therapeutics, but such potency has been achieved. Just as the design of organic chemotherapeutics have shifted from potent alkylators and other inhibitors of DNA synthesis to far more tai-

lored, subtle reagents, the design of novel metallotherapeutics now requires a targeted approach. There has been a paradigm shift in next generation chemotherapeutic drug design that focuses on specifically tailored therapies. The unique reactivity and coordination geometry of metal complexes make them the ideal scaffold for this new tailor-made design of targeted therapeutics. The examples discussed herein exemplify the enormous potential of this new strategy in transition metal chemotherapy and perhaps lay the groundwork for this burgeoning new field.

1.7 References

- 1 Mansour, V. H.; Rosenberg, B.; Vancamp, L.; Trosko, J. E. *Nature* **1969**, *222*, 385–386.
- 2 Wheate, N. J.; Walker, S.; Craig, G. E.; Oun, R. *Dalton Trans.* **2010**, *39*, 8113–8127
- 3 Kelland, L. R.; Sharp, S. Y.; O’Neill, C. F.; Raynaud, F. I.; Beale, P. J.; Judson, I. *R. J. Inorg. Biochem.* **1999**, *77*, 111–115.
- 4 Jamieson, E. R.; Lippard, S. J. *Chem. Rev.* **1999**, *99*, 2467-2498.
- 5 Wang, D.; Lippard, S. J. *Nat. Rev. Drug Discovery* **2005**, *4*, 307–320.
- 6 Dulhunty, A. F. *J. Physiol.* **1978**, *276*, 67-82.
- 7 Zhang, C. X.; Lippard, S. J. *Curr. Opin. Chem. Biol.* **2003**, *7*, 481-489.
- 8 Siddik, Z. H. *Oncogene* **2003**, *22*, 7265-7279.
- 9 Selvakumaran, M.; Pisarcik, D. A.; Bao, R.; Yeung, A. T.; Hamilton, T. C. *Cancer Res.* **2003**, *63*, 1311-1316.
- 10 Ferry, K. V.; Hamilton, T. C.; Johnson, S. W. *Biochem. Pharmacol.* **2000**, *60*, 1205-1313.
- 11 Johnson, S. W.; Perez, R. P.; Godwin, A. K.; Yeung, A. T.; Handel, L. M.; Ozols, R. F.; Hamilton, T. C. *Biochem. Pharmacol.* **1994**, *47*, 689-697.
- 12 Huang, J.-C.; Zamble, D. B.; Reardon, J. T.; Lippard, S. J.; Sancar, A. *Proc. Natl. Acad. Sci. U.S.A.* **1994**, *91*, 10394-10398.
- 13 McA’Nulty, M. M.; Lippard, S. J. *Mutat. Res., DNA Repair* **1996**, *362*, 75-86.

- 14 Aebi, S.; Kurdi-Haidar, B.; Gordon, R.; Cenni, B.; Zheng, H.; Fink, D.; Christen, R. D.; Boland, R.; Koi, M.; Fishel, R.; Howell, S. B. *Cancer Res.* **1996**, *56*, 3087-3090.
- 15 Fink, D.; Nebel, S.; Aebi, S.; Zheng, H.; Cenni, B.; Nehme, A.; Christen, R. D.; Howell, S. B. *Cancer Res.* **1996**, *56*, 4881-4886.
- 16 Rhyu, M. S. *J. Natl. Cancer Inst.* **1996**, *88*, 240-251.
- 17 Kehe, K.; Szinicz, L. *Toxicology* **2005**, *214*, 198-209.
- 18 Montana, A. M.; Batalla, C. *Curr. Med. Chem.* **2009**, *16*, 2235-2260.
- 19 Niedle, S.; Ismail, I. M.; Sadler, P. J. *J. Inorg. Biochem.* **1980**, *13*, 205-212.
- 20 Frey, U.; Ranford, J. D.; Sadler, P. J. *Inorg. Chem.* **1993**, *32*, 1333-1340.
- 21 Boulikas, T.; Vougiouka, M. *Oncol. Rep.* **2003**, *10*, 1663-1682.
- 22 Kasparikova, J.; Vojtiskova, M.; Natile, G.; Brabec, V. *Chem. Eur. J.* **2008**, *14*, 1330-1341.
- 23 Ibrahim, A.; Hirschfeld, S.; Cohen, M. H.; Griebel, D. J.; Williams, G. A.; Pazdur, R. *Oncologist* **2004**, *9*, 8-12.
- 24 Hall, M. D.; Mellor, H. R.; Callaghan, R.; Hambley, T. W. *J. Med. Chem.* **2007**, *50*, 3403-3410.
- 25 Johnstone, T. C.; Wilson, J. J.; Lippard, S. J. *Inorg. Chem.* **2013**, *52*, 12234-12249.
- 26 Perez, J. M.; Fuertes, M. A.; Alonso, C.; Navarro-Ranninger, C. *Crit. Rev. Oncol. Hematol.* **2000**, *35*, 109-120.
- 27 Ang, W. H.; Dyson, P. J. *Eur. J. Inorg. Chem.* **2006**, 4003-4018.

- 28 Beltran, B., Casado, P., Rodríguez-Prados, J.-C., Cutillas, P. R. *J. Proteomics* **2012**, *77*, 492–503.
- 29 Feng, L. et al. *J. Am. Chem. Soc.* **2011**, *133*, 5976–5986.
- 30 Kunick, C., Ott, I. *Angew. Chem. Int. Ed.* **2010**, *49*, 5226–5227.
- 31 Koblinski, J. E., Ahram, M., Sloane, B. F. *Clin. Chim. Acta* **2000**, *291*, 113–135.
- 32 Meggers, E. *Chem. Commun.* **2009**, 1001–1010.
- 33 Casini, A. et al. *J. Med. Chem.* **2008**, *51*, 6773–6781.
- 34 Guidi, F., et al. *J. Inorg. Biochem.* **2013**, *118*, 94–99.
- 35 Holst, F. et al. *Nat. Genet.* **2007**, *39*, 655–660.
- 36 Vessières, A., Top, S., Beck, W., Hillard, E., Jaouen, G. *Dalton Trans.* **2006**, 529–541.
- 37 Pigeon, P., Top, S., Vessières, A., Huché, M., Hillard, E., Salomon, E., Jaouen, G. *J. Med. Chem.* **2005**, *48*, 2814–2821.
- 38 Gogvadze, V., Orrenius, S., Zhivotovsky, B. *Trends Cell Biol.* **2008**, *18*, 166–173.
- 39 Wisnovsky, S. P., Wilson, J. J., Radford, R. J., Pereira, M. P., Laposa, R. R., Lippard, S. J., Kelley, S. O. *Chem. Biol.* **2013**, *20*, 1–6.
- 40 Lo, K. K.-W.; Choi, A. W.-T.; Law, W. H.-T. *Dalton Trans.* **2012**, *41*, 6021-6047.
- 41 Eriksson, M.; Leijon, M.; Hiort, C.; Norden, B.; Graslund, A. *Biochemistry* **1994**, *33*, 5031–5040.
- 42 Meijler, M. M.; Zelenko, O.; Sigman, D. S. *J. Am. Chem. Soc.* **1997**, *119*, 1135–1136.

- 43 Chen, C. H. B.; Milne, L.; Landgraf, R.; Perrin, D. M.; Sigman, D. S. *Chembiochem.* **2001**, *2*, 735–740.
- 44 Barton, J. K. *Science* **1986**, *233*, 727-734.
- 45 Erkkila, K. E.; Odom, D. T.; Barton, J. K. *Chem. Rev.* **1999**, *99*, 2777–2795.
- 46 Zeglis, B. M.; Pierre, V. C.; Barton, J. K. *Chem. Comm.* **2007**, *44*, 4565-4579.
- 47 Suh, D.; Chaires, J. B. *Bioorg. Med. Chem.* **1995**, *3*, 723-728.
- 48 Kielkopf, C. L.; Erkkila, K. E.; Hudson, B. P.; Barton, J. K.; Rees, D. C. *Nature Struct. Biol.* **2000**, *7*, 117–121.
- 49 Friedman, A. E.; Chambron, J. C.; Sauvage, J. P.; Turro, N. J.; Barton, J. K. *J. Am. Chem. Soc.* **1990**, *112*, 4960–4962.
- 50 Turro, C.; Bossmann, S. H.; Jenkins, Y.; Barton, J. K.; Turro, N. J. *J. Am. Chem. Soc.* **1995**, *117*, 9026–9032.
- 51 Olson, E. J. C.; Hu, D.; Hormann, A.; Jonkman, A. M.; Arkin, M. R.; Stemp, E. D. A.; Barton, J. K.; Barbara, P. F. *J. Am. Chem. Soc.* **1997**, *119*, 11458–11467.
- 52 Puckett, C. A.; Barton, J. K. *J. Am. Chem. Soc.* **2007**, *129*, 46–47.
- 53 McConnell, A. J.; Lim, M. H.; Olmon, E. D.; Song, H. Dervan, E. E.; Barton, J. K. *Inorg. Chem.* **2012**, *51*, 12511-12520.
- 54 Sitlani, A.; Long, E. C.; Pyle, A. M.; Barton, J. K. *J. Am. Chem. Soc.* **1992**, *114*, 2303–2312.
- 55 Hartshorn, R. M.; Barton, J. K. *J. Am. Chem. Soc.* **1992**, *114*, 5919–5925.
- 56 Boerner, L. J. K.; Zaleski, J. M. *Curr. Opin. Chem. Biol.* **2005**, *9*, 135-144
- 57 Núñez, M. E.; Barton, J. K. *Curr. Opin. Chem. Biol.* **2000**, *4*, 199-206.
- 58 Krotz, A. H.; Hudson, B. P.; Barton, J. K. *J. Am. Chem. Soc.* **1993**, *115*,

- 12577–12578.
- 59 Jackson, B. A.; Barton, J. K. *J. Am. Chem. Soc.* **1997**, *119*, 12986–12987.
- 60 Isaacs, R. J.; Rayens, W. S.; Spielmann, H. P. *J. Mol. Biol.* **2002**,
319, 191–207.
- 61 Peyret, N.; Seneviratne, P. A.; Allawi, H. T.; SantaLucia, J. *Biochemistry* **1999**,
38, 3468–3477.
- 62 Cordier, C.; Pierre, V. C.; Barton, J. K. *J. Am. Chem. Soc.* **2007**, *129*, 12287–
12295.
- 63 Zeglis, B. M.; Pierre, V. C.; Kaiser, J. T.; Barton, J. K. *Biochemistry* **2009**, *48*,
4247–4253.
- 64 Lerman, L. S. *J. Mol. Biol.* **1961**, *3*, 18–30.
- 65 Murner, H.; Jackson, B. A.; Barton, J. K. *Inorg. Chem.* **1998**, *37*,
3007–3012.
- 66 Jackson, B. A.; Alekseyev, V. Y.; Barton, J. K. *Biochemistry* **1999**, *38*, 4655–
4662.
- 67 Peyret, N.; Seneviratne, P. A.; Allawi, H. T.; SantaLucia, J. *Biochemistry* **1999**,
38, 3468–3477.
- 68 Jackson, B. A.; Barton, J. K. *Biochemistry* **2000**, *39*, 6176–6182.
- 69 Pierre, V. C.; Kaiser, J. T.; Barton, J. K. *Proc. Natl. Acad. Sci. U.S.A.* **2007**, *104*,
429–434.
- 70 Song, H. Kaiser; J. T.; Barton, J. K. *Nature Chem.* **2012**, *4*, 615–620.
- 71 Loeb, L. A. *Cancer Res.* **2001**, *61*, 3230–3239.

- 72 Bhattacharya, N. P.; Skandalis, A.; Ganesh, A.; Groden, J.; Meuth, M. *Proc. Natl. Acad. Sci. U.S.A.* **1994**, *91*, 6319–6323.
- 73 Iyer, R. R.; Pluciennik, A.; Burdett, V.; Modrich, P. L. *Chem. Rev.* **2006**, *106*, 302–323.
- 74 Carethers, J. M.; Hawn, M. T.; Chauhan, D. P.; Luce, M. C.; Marra, G.; Koi, M.; Boland, C. R. *J. Clin. Invest.* **1996**, *98*, 199–206.
- 75 Hart, J. R.; Glebov, O.; Ernst, R. J.; Kirsch, I. R.; Barton, J. K. *Proc. Natl. Acad. Sci. U.S.A.* **2006**, *103*, 15359–15363.
- 76 Ernst, R. J.; Song, H.; Barton, J. K. *J. Am. Chem. Soc.* **2009**, *131*, 2359–2366.
- 77 Ernst, R. J.; Komor, A. C.; Barton, J. K. *Biochemistry* **2011**, *50*, 10919–10928.
- 78 Komor, A. C.; Schneider, C. J.; Weidmann, A. G.; Barton, J. K. *J. Am. Chem. Soc.* **2012**, *134*, 19223–19233.
- 79 Weidmann, A. G.; Komor, A. C.; Barton, J. K. *Philos. Trans. R. Soc. A.* **2013**, *371*, 20120117.
- 80 Koi, M.; Umar, A.; Chauhan, D. P.; Cherian, S. P.; Carethers, J. M.; Kunkel, T. A.; Boland, C. R. *Cancer Res.* **1994**, *54*, 4308-4312.
- 81 Bailis, J. M.; Gordon, M. L.; Gurgel, J. L.; Komor, A. C.; Barton, J. K.; Kirsch, I. R. *PLoS One* **2013**, *8*, e78726.
- 82 Komor, A. C.; Barton, J. K. *J. Am. Chem. Soc.* **2014**, *136*, 14160-14172.
- 83 Schatzschneider, U.; Barton, J. K. *J. Am. Chem. Soc.* **2004**, *126*, 8630–8631.
- 84 Lim, M. H.; Lau, I. H.; Barton, J. K. *Inorg. Chem.* **2007**, *46*, 9528–9530.
- 85 Petitjean, A.; Barton, J. K. *J. Am. Chem. Soc.* **2004**, *126*, 14728–14729.
- 86 Ernst, R. J. *Unpublished results.*

- 87 Frankel, A. D.; Pabo, C. O. *Cell* **1988**, *55*, 1189-1193
- 88 Brunner, J.; Barton, J. K. *Biochemistry* **2006**, *45*, 12295–12302.
- 89 Homesley, H. D.; Bundy, B. N.; Hurteau, J. A.; Roth, L. M. *Gynecol. Oncol.* **1999**, *72*, 131-137.